nature nanotechnology

LETTERS

PUBLISHED ONLINE: 23 JANUARY 2011 | DOI: 10.1038/NNANO.2010.278

# Designed ultrafast optical nonlinearity in a plasmonic nanorod metamaterial enhanced by nonlocality

G. A. Wurtz[1], R. Pollard[2], W. Hendren[2], G. P. Wiederrecht[3], D. J. Gosztola[3], V. A. Podolskiy[4] and A. V. Zayats[5]*

**All-optical signal processing enables modulation and transmission speeds not achievable using electronics alone[1,2]. However, its practical applications are limited by the inherently weak nonlinear effects that govern photon–photon interactions in conventional materials, particularly at high switching rates[3]. Here, we show that the recently discovered nonlocal optical behaviour of plasmonic nanorod metamaterials[4] enables an enhanced, ultrafast, nonlinear optical response. We observe a large (80%) change of transmission through a subwavelength thick slab of metamaterial subjected to a low control light fluence of 7 mJ cm$^{-2}$, with switching frequencies in the terahertz range. We show that both the response time and the nonlinearity can be engineered by appropriate design of the metamaterial nanostructure. The use of nonlocality to enhance the nonlinear optical response of metamaterials, demonstrated here in plasmonic nanorod composites, could lead to ultrafast, low-power all-optical information processing in subwavelength-scale devices.**

An increased photon–photon interaction and, consequently, the nonlinear optical response, can be facilitated through the use of metals as active media. The metal in such an arrangement has three roles. First, by coupling light to the collective free electron motion near a metal surface (so-called surface plasmons), enhancement of the electromagnetic field is achieved, which is crucial for the observation of nonlinear interactions that are superlinearly dependent on the field strength[5,6]. The best known example of this effect is surface-enhanced Raman scattering, which demonstrates single-molecule sensitivity[7]. Second, plasmonic excitations are extremely sensitive to the permittivity of the metal and the adjacent dielectric—a property widely used in plasmonic-based bio- and chemosensors[8]. Third, the temporal behaviour of the optical properties of metals is very fast, ranging from tens of femtoseconds to a few picoseconds in different regimes, depending on the electron plasma relaxation processes involved[9,10]. These characteristics make plasmonic structures very promising for ultrafast all-optical applications at low light intensities.

To observe a sizable nonlinear optical effect while also preventing excessive heat transfer (leading to increased relaxation times and possible structural damage), plasmonic nanostructures are often hybridized with nonlinear dielectrics to lower the required control light power. Modulation, switching and bistability have been demonstrated in both continuous-wave (c.w.) and pulsed regimes in all-optically controlled plasmonic nanostructures[11–20]. However, in bare plasmonic nanostructures, the observed nonlinearity has usually been relatively small and has required significant control light powers. Notable exceptions include a 35% signal modulation with 13 mJ cm$^{-2}$ pump fluence using an interband transition in aluminium[21] and a 60% signal modulation with 60 mJ cm$^{-2}$ pump fluence for coupling of light to surface plasmon polaritons using diffraction gratings and interband transitions in gold[22]. A signal modulation saturated at ~20% at a fluence of 1.6 mJ cm$^{-2}$ has been achieved in a silicon-silver fishnet metamaterial using excitation of free carriers in silicon[23].

We show that the nonlinear response of plasmonic metamaterials can be significantly enhanced if the metamaterial is designed such that the electric field at one position within the metamaterial affects the polarization at a different position. This nonlocal response is described by wave vector-dependent permittivity[4]. The nonlocality of the longitudinal plasmon modes in the nanorod metamaterial results in anomalously large changes in the optical density (ΔOD) of up to 0.7 (a change in transmission as high as 80%). These dramatic changes occur at the subpicosecond timescale and with relatively weak peak pump intensity on the order of 10 GW cm$^{-2}$, corresponding to a fluence of 7 mJ cm$^{-2}$. This results in $\Delta OD/OD = 0.44$, a significant increase over the previously observed values of $\Delta OD/OD \approx 0.1$ for low-concentration, non-interacting gold nanorods and smooth gold films[15,19,20]. Both spectral response and dynamic response can be engineered by choosing appropriate nanorod metamaterial parameters, such as nanorod diameter and length and the separation between the nanorods in the assembly.

The linear optical response of the plasmonic nanorod metamaterials shown in Fig. 1 (see Supplementary Information for details of fabrication) is governed by the interaction between surface plasmon excitations of closely spaced nanorods[24–27]. The optical density spectra $OD = -\log_{10}(T/T_0)$, where $T$ is the zero-order transmittance of an assembly of gold nanorods and $T_0$ is the reference transmittance, reveal two dominating resonances with different angular and polarization dependences. The position of the resonances depends on the rod length, diameter and inter-rod distance. The transverse (T) resonance is associated with the quasistatic plasmonic excitations along the short axis of the rods and is related to the modes supported by individual nanorods[24,25].

The longitudinal (L) resonance results from the coupling between the dipolar plasmonic modes parallel to the nanorod long axis. As the result of strong coupling between the nanorods, individual plasmonic modes are combined into two transverse-magnetic (TM) waves, supported by the nanorod metamaterial.

[1]Department of Physics, University of North Florida, Jacksonville, Florida 32224, USA, [2]Centre for Nanostructured Media, The Queen's University of Belfast, Belfast BT7 1NN, UK, [3]Center for Nanoscale Materials, Argonne National Laboratory, Argonne, Illinois 60439, USA, [4]Department of Physics and Applied Physics, University of Massachusetts, Lowell, Massachusetts 01854, USA, [5]Department of Physics, King's College London, Strand, London WC2R 2LS, UK. *e-mail: a.zayats@kcl.ac.uk

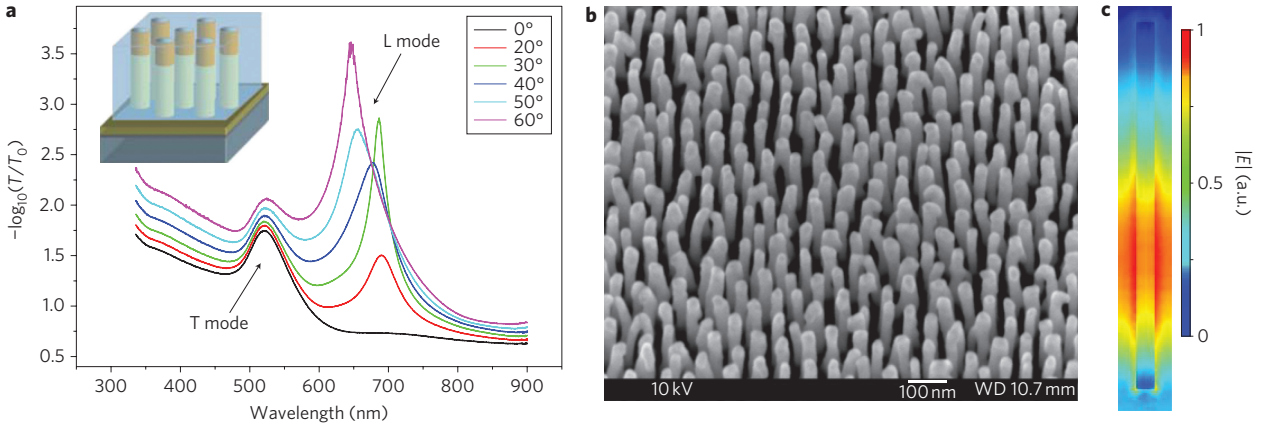


**Figure 1 | Plasmonic nanorod metamaterial and its optical properties. a**, Angle-dependent zero-order linear extinction of an array of gold nanorods embedded in an alumina matrix. The rods are attached vertically to a glass substrate and have an average length, diameter and centre-to-centre spacing of 400 nm, 20 nm and 70 nm, respectively. Illuminating light is TM-polarized. **b**, Scanning electron microscopy image of the nanorod assembly. For imaging, the matrix was removed. Scale bar is 100 nm. **c**, Numerically calculated distribution of the electric field amplitude for strongly interacting gold rods. The metamaterial parameters are as in **a**. Illumination field is TM-polarized and incident from the substrate side at an angle of 45° in air.

The properties of these waves depend on both the geometry of the metamaterial and its losses, and can be adequately described by a nonlocal effective medium theory[4]. This nonlocality, that is, the dependence of the effective permittivity on the wave vector, appears on the macroscopic (metamaterial) scale, whereas the response of each constituent of the metamaterial is local. Note that the extinction nature in the vicinity of L resonance is fundamentally different from that at T resonance. While the latter is solely related to material absorption, the former is primarily governed by the interference of two TM-polarized modes (a maximum OD corresponds to destructive interference between two waves at the exit side of the metamaterial[4]). These nonlocality-induced resonances have a non-trivial dependence on the angle of incidence of the probe light and, as in any interference process, are extremely sensitive to variations in the material and the geometric characteristics of the system. This means that the spectral properties of these resonances can be designed to a great extent by adjusting the geometrical parameters of the metamaterials (nanorod diameters, nanorod separations or nanorod length; see Supplementary Information). Tunability ranges from ~550 nm in the visible to near-infrared wavelengths[26,28].

To study the optical nonlinear response of the metamaterial, we performed transient extinction spectroscopy measurements (for details, see Supplementary Information). The transient extinction spectrum $\Delta OD = -\log_{10}(T_{ON}/T_{OFF})$ for TM-polarized probe light, where $T_{ON}$ is the transmission of the sample at the delay time $\tau$ following excitation by the pump beam and $T_{OFF}$ is the transmission of the sample in the ground state (that is, when $\tau \rightarrow \infty$), is mapped in Fig. 2a for an angle of incidence of 20°. Several cross-sections of the transient response map are shown in Fig. 2b as a function of time delay, and Fig. 2c presents the angular dependence of the transient spectra for a pump–probe time delay of $\tau = 600$ fs. The control light ($\lambda = 465$ nm, $\Delta\tau = 130$ fs) has a peak intensity of ~1 GW cm$^{-2}$ (note that at this wavelength and angle of incidence ~3% of the control light is absorbed by the structure). This is well within the low excitation regime, where the pump energy is mostly transferred to the electronic modes of the rods and then coupled to available electron and phonon modes within the rods and to the dielectric environment[29,30]. The magnitude of ΔOD was found to vary from 0.0015 at a peak intensity of 0.2 GW cm$^{-2}$ (42 nJ energy per pulse) to 0.7 at 11 GW cm$^{-2}$ (2.4 μJ energy per pulse). Remarkably, the ΔOD of 0.7 corresponds to an 80% change in transmission with a 130 fs pulse-width-limited rise time and a recovery time of less than 2 ps. This corresponds to a ΔOD/OD ratio of ~0.4 calculated using the extinction OD = 2.3 obtained at the 40° angle of incidence and accounting for the background OD of 0.7 due to defect scattering and/or other uncontrollable effects.

The dynamics of the spectral response observed in Fig. 2a is specific to the plasmonic resonances of the assembly. Although the behaviour of the T mode is typical of a localized mode for which the plasmon resonance overlaps interband transitions[29,30], the behaviour of the L mode is more complex. As a general trend, this resonance demonstrates a dispersive-type behaviour resulting from modifications in the linewidth and spectral position of the L mode, both of which are also typical of isolated plasmonic resonances in the absence of strong damping due to interband scattering[16,31]. However, while the isolated plasmonic systems would not show any angular dependence for the dispersive behaviour, the L mode shows drastic changes in its transient spectral response with angle of incidence, as shown in Fig. 2c. This strong variation of the transient response is a direct consequence of interference-governed transmission through nonlocal media. The deviation from the conventional behaviour occurs for all time delays at the incidence angle where spectral changes related to nonlocal effects in the metamaterial are most notable (cf. Figs 1a and 2c). This angular dependence of the spectral changes resulting from nonlocal effects in the metamaterial is reproduced well using both nonlocal effective medium modelling and finite-element numerical simulations (Fig. 2d). The modifications of the dielectric constant of gold under excitation were calculated using the Drude–Lorentz model with random phase approximation to account for permittivity changes due to the variations in electron temperature under the influence of the control beam (see Supplementary Information). The main contribution to the observed nonlinear response was found to originate from an increase in the intraband damping constant, leading to modification of both the real and imaginary parts of the metal's permittivity, with the increase in $\mathrm{Im}(\varepsilon_{Au})$ being the most significant contribution to the changes in the spectral range of the TM modes. The associated increase in material losses results in modification of the nonlocal optical response of the metamaterial, which is extremely sensitive to losses in the metal, as has been reported previously[4]. It should be emphasized that the interplay between nonlocality and losses is the mechanism that allows one to achieve both strong suppression and enhancement of the transmission in different spectral ranges. With an increase in the control light intensity, the L-mode nonlinear changes become dominant (Figs 2e,f, 3a), because stronger modification of the nonlocal response takes place (more significant changes in Imε). Model

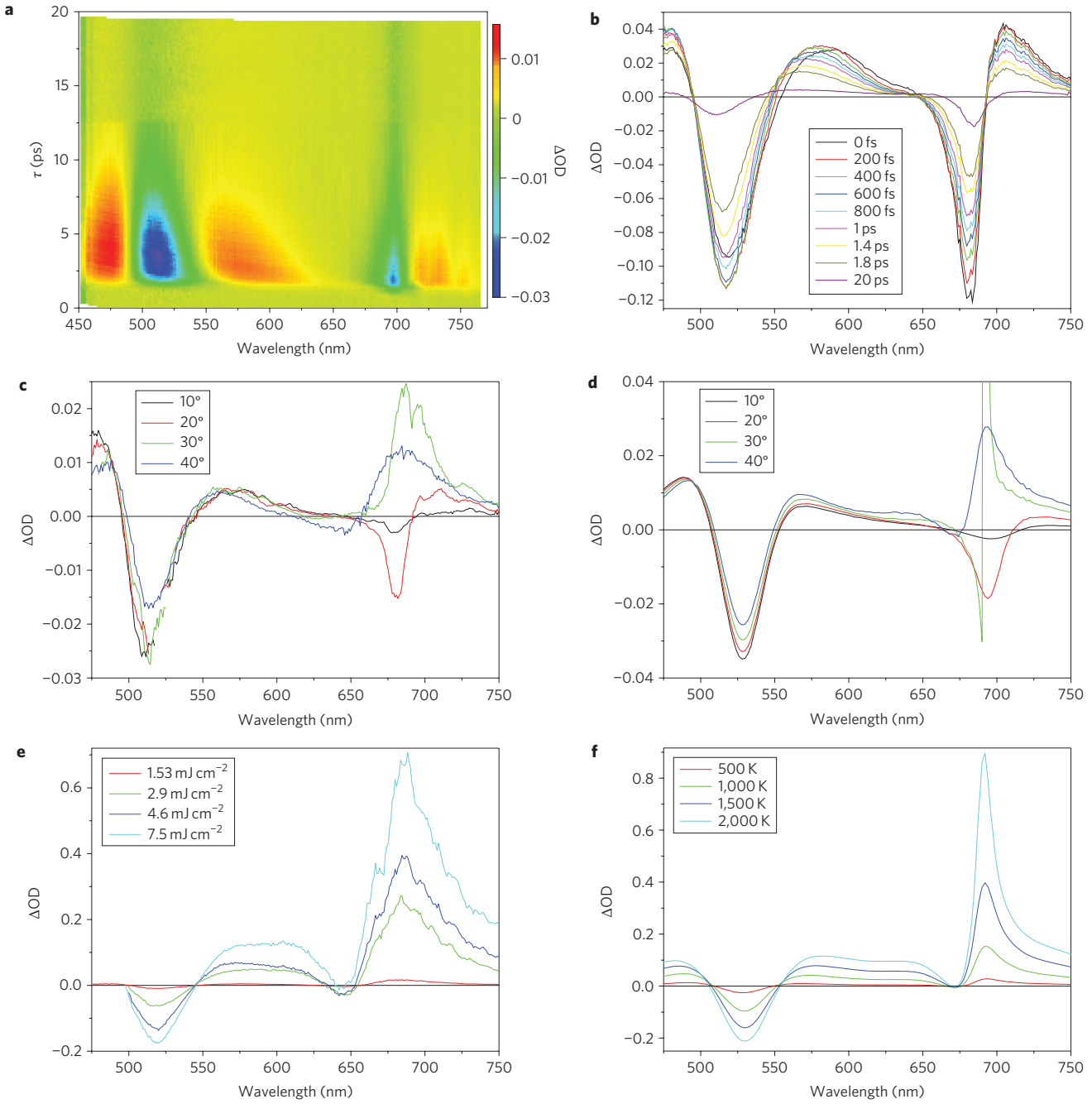


**Figure 2 | Modifications of the optical properties of the metamaterial under control light illumination. a**, Transient extinction map measured for the arrays of gold rods in Fig. 1a for TM-polarized probe light at an angle of incidence of 20°. Pump wavelength is 465 nm; fluence is 0.7 mJ cm$^{-2}$. **b**, Transient extinction spectra at various time delays between pump and probe beams. Spectrum '0 fs' corresponds to the spectrum of the metamaterial measured directly after optical pumping. The other transient spectra correspond to increasing pump–probe time delays, $\tau$. **c**, Transient extinction spectra at $\tau = 600$ fs measured for different angles of incidence. **d**, Numerically modelled transient extinction spectra corresponding to the experimental situation in **c** with an electron temperature increase to 500 K following control light absorption, corresponding to $\Delta\mathrm{Im}\varepsilon/\mathrm{Im}\varepsilon \approx 0.01$; $\Delta\mathrm{Re}\varepsilon/\mathrm{Re}\varepsilon$ is negligible far from the interband transition (see Supplementary Information for details). **e**, Transient extinction measured for different pump fluences. **f**, Transient extinction calculated for different electron temperatures. In both **e** and **f**, angle of incidence is 40° and probe light is TM-polarized. Model spectra were calculated without any fitting parameters and do not account for the angular divergence of the probe beam and possible deviations in the angle of incidence.

calculations reproduce all the experimental behaviour, but with much sharper spectral features, despite the fact that the linear spectra are reproduced completely by the model.

Figure 3a highlights the significant impact of nonlocality on the magnitude of the transient response of the structure. Here, the maximum of the change in transmission for both the T and L modes is plotted together with their relative extinction as a function of pump fluence, showing that nonlocal effects lead to an almost 400% stronger nonlinear response of the L mode compared to the T mode. The drastic differences in ΔOD dependences for T and L modes arise from the fundamentally different physics behind the transmission through the local (T) and nonlocal (L) modes supported by the metamaterial. The influence of small variations in Imε on the transmission are enhanced in the vicinity of L

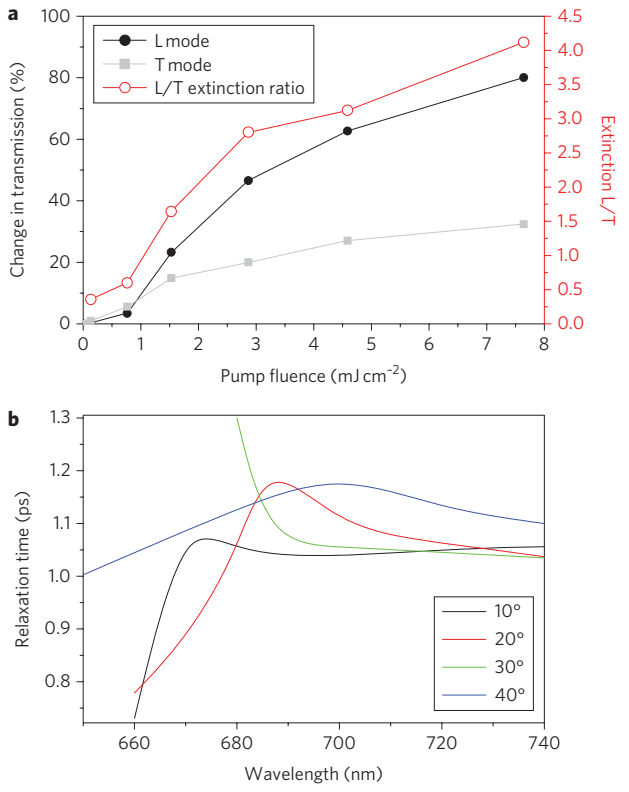


**Figure 3 | Intensity, spectral and angular dependences of the transient optical response of the metamaterial. a**, Percent changes in the optical transmission measured from the transient signal of the array of plasmonic nanorods for the T mode (grey curve) and L mode (black curve) as a function of pump fluence. The absolute ratio between L mode and T mode transient extinctions is also shown (red curve). The probe light is TM-polarized and incident on the sample at an angle of 40°. **b**, Wavelength dependence of $\tau_{\text{L-mode}}$ relaxation time for different angles of incidence. Pump fluence is 0.7 mJ cm$^{-2}$.

resonance due to the interference of the two TM modes in the nonlocal metamaterial.

The time response of the T mode follows a behaviour similar to isolated plasmonic resonances supported by subwavelength-sized gold particles. Its response is mainly governed by non-radiative processes, with a spectral shape dominated by a transient bleach at ~515 nm surrounded by induced absorption wings (Fig. 2b). This peculiar shape is associated with the change in dielectric constant of gold as a function of electron temperature. (See Supplementary Information for a detailed discussion of electron thermalization processes.) From the transient spectra of Fig. 2a, it can be seen that the relaxation dynamics of the T mode is governed by two relaxation channels corresponding to electron–phonon and phonon–phonon scattering: $\gamma_{\text{T-mode}} = 1/\tau_{\text{T-mode}} = 1/\tau_{\text{e-ph}} + 1/\tau_{\text{ph-ph}}$ where $\tau_{\text{e-ph}} = 1.6 \pm 0.05$ ps and $\tau_{\text{ph-ph}} = 115 \pm 0.1$ ps, respectively.

The dynamics of the L mode displays a similar behaviour, with most of the energy dissipated within the picosecond timescale, where electron–electron scattering and phonon–phonon scattering events are not predominant relaxation pathways. However, compared to the T mode, the L mode demonstrates an enhanced relaxation rate with $\gamma_{\text{L-mode}} > \gamma_{\text{T-mode}}$, which is unexpected for a plasmonic resonance in this spectral range. Indeed, considering the spectral position of the L mode around 1.8 eV (690 nm), well below the interband transition threshold of 2.4 eV, no contributions from those transitions are expected in the picosecond timescale. The dynamics of the L mode in the picosecond range must therefore comprise an additional relaxation channel identified as the waveguided mode[27] and can be described by $\tau_{\text{L-mode}} = (\gamma_{\text{L-mode}})^{-1} = (\gamma_{\text{e-ph}} + \gamma_{\text{Wg}})^{-1}$. The values of $\tau_{\text{L-mode}}$ ranging from $0.76 \pm 0.05$ ps to $1.13 \pm 0.05$ ps were measured for different wavelengths around the resonance (Fig. 2a), resulting in a non-uniform modification of the resonance shape with delay time. A similar dynamic behaviour is also observed for other angles of incidence with an increase in the average relaxation time for larger angles, mostly due to an increased extinction of the mode ($\tau_{\text{L-mode}}$ increase is ~10% when the angle varies from 10° to 40°). Most importantly, the dynamics of the L mode is consistently faster than that measured for the T mode (Fig. 3b), especially at higher pump fluencies. Again, this is quite surprising, considering that the L mode does not overlap interband transitions and has a ~50% smaller linewidth than the T mode. Both effects are usually related, leading to longer relaxation times of the long-wavelength resonance compared to its shorter-wavelength relative. This is not observed for the L mode, which is associated with a plasmonic mode delocalized over the nanorod assembly. Based on the dynamics of the T mode taken here as a reference, the extra decay channel $\gamma_{\text{Wg}}$ for the L mode reflects coupling to the pseudo-waveguided mode with a rate $\gamma_{\text{Wg}} = (2.4\ \text{ps})^{-1}$ at a wavelength of 707 nm (Fig. 2b). A simplified schematic of the L mode relaxation pathways occurring in the picosecond time range is shown in Supplementary Fig. S2. A reduction in pump fluence to 0.7 mJ cm$^{-2}$ leads to a faster ~700 fs relaxation time (Fig. 3b) due to a smaller increase of the electron temperature[29,30].

In conclusion, we have demonstrated a plasmonic metamaterial showing ultrafast subpicosecond response times and anomalously high changes in optical density that occur under optical excitation. Absolute ΔOD changes of up 0.7 were observed, corresponding to 80% change in transmission of the metamaterial with a subpicosecond recovery time. The experimental results suggest that 20% transmission modulation is achievable in 100 × 100 nm$^2$ devices with ~2 fJ energy per pulse and 80% modulation with ~20 fJ. Experiments and modelling strongly suggest that both this anomalously large response and its ultrafast recovery time are due to the nonlocal nature of the plasmonic mode of the metamaterial, so that small changes in permittivity under excitation modify the nonlocal response, which in turn leads to strong changes in transmission. Because the strongly nonlinear spectral and kinetic behaviour observed for the nonlocal L mode relative to the localized T mode can be specifically engineered for a required wavelength range by changing the nanostructure parameters, these metamaterials provide a new class of optical media for achieving ultrafast highly nonlinear processes, with numerous applications in optical communications, extraordinarily sensitive optical spectroscopies and subwavelength imaging technologies. Coupled plasmonic nanoparticles have also been proposed as a means to propagate energy through linear chains of closely coupled nanoparticle chains, while still maintaining subwavelength lateral widths[27,32]. In this context, the nonlinear response of the delocalized L mode may provide a basis for the comprehensive design of the next generation of nanophotonic circuitry. As the extinction, to a large extent, is associated with coupling to the longitudinal waveguided mode, the strongest nonlinear response associated with the maximum of the extinction seems to be perfectly suitable for designing integrated switches. In all these applications, the ability to switch and modulate optical properties, or indeed tune the properties of the nanostructures with the control optical beam, will be of great importance.

Received 2 August 2010; accepted 10 December 2010; published online 23 January 2011

## References

1. Gibbs, H. M. *Optical Bistability: Controlling Light with Light* (Academic, 1985).
2. Almeida, V. A., Barrios, C. A., Panepucci, R. R. & Lipson, M. All-optical control of light on a silicon chip. *Nature* **431,** 1081–1084 (2004).

3. Boyd, R. W. *Nonlinear Optics* (Academic, 2003).
4. Pollard, R. J. *et al.* Optical nonlocalities and additional waves in epsilon-near-zero metamaterials. *Phys. Rev. Lett.* **102,** 127405 (2009).
5. Raether, H., *Surface Plasmons on Smooth and Rough Surfaces and on Gratings* (Springer, 1987).
6. Zayats, A. V., Smolyaninov, I. I. & Maradudin, A. A. Nano-optics of surface plasmon polaritons. *Phys. Rep.* **408,** 131–314 (2005).
7. Nie, S. & Emory, S. R. Probing single molecules and single nanoparticles by surface-enhanced Raman scattering. *Science* **275,** 1102–1106 (1997).
8. Anker, J. N. *et al.* Biosensing with plasmonic nanosensors. *Nat. Mat.* **7,** 442–453 (2008).
9. Sun, C. K., Vallée, F., Acioli, L., Ippen, E. P. & Fujimoto, J. G. Femtosecond investigation of electron thermalization in gold. *Phys. Rev. B* **48,** 12365–12368 (1993).
10. Fatti, N. D., Bouffanais, R., Vallée, F. & Flytzanis, C. Nonequilibrium electron interactions in metal films. *Phys. Rev. Lett.* **81,** 922–925 (1998).
11. Pacifici, D., Lezec, H. J. & Atwater, H. A. All-optical modulation by plasmonic excitation of CdSe quantum dots. *Nature Photon.* **1,** 402–406 (2007).
12. Pala, R. A., Shimizu, K. T., Melosh, N. A. & Brongersma, M. L. A nonvolatile plasmonic switch employing photochromic molecules. *Nano Lett.* **8,** 1506–1510 (2008).
13. Smolyaninov, I. I., Davis, C. C. & Zayats, A. V. Light-controlled photon tunneling. *Appl. Phys. Lett.* **81,** 3314–3316 (2002).
14. Wurtz, G. A., Pollard R. & Zayats, A. V. Optical bistability in nonlinear surface plasmon polaritonic crystals. *Phys. Rev. Lett.* **97,** 057402 (2006).
15. Rotenberg, N., Betz, M. & van Driel, H. M. Ultrafast control of grating-assisted light coupling to surface plasmons. *Opt. Lett.* **33,** 2137–2139 (2008).
16. Varnavski, O. P., Goodson, T., Mohamed, M. B. & El-Sayed, M. A. Femtosecond excitation dynamics in gold nanospheres and nanorods. *Phys. Rev. B* **72,** 235405 (2005).
17. Perner, M., Gresillon, S., März, J., von Plessen, G. & Feldmann, J. Observation of hot-electron pressure in the vibration dynamics of metal nanoparticles. *Phys. Rev. Lett.* **85,** 792–795 (2000).
18. Wurtz, G. A. & Zayats, A. V. Nonlinear surface plasmon polaritonic crystals. *Laser Photon. Rev.* **2,** 125–135 (2008).
19. MacDonald, K. F., Samson, Z. L., Stockman, M. I. & Zheludev, N. I. Ultrafast active plasmonics. *Nature Photon.* **3,** 55–58 (2009).
20. Link, S., Burda, C., Mohamed, M. B., Nikoobakht, B. & El-Sayed, M. A. Femtosecond transient-absorption dynamics of colloidal gold nanorods: shape independence of the electron–phonon relaxation time. *Phys. Rev. B* **61,** 6086–6090 (2000).
21. Samson, Z. L., MacDonald, K. F. & Zheludev, N. I. Femtosecond active plasmonics: ultrafast control of surface plasmon propagation. *J. Opt. A* **11,** 114031 (2009).
22. Rotenberg, N., Caspers, J. N. & van Driel, H. M. Tunable ultrafast control of plasmonic coupling to gold films. *Phys. Rev. B* **80,** 245420 (2009).
23. Dani, K. *et al.* Subpicosecond optical switching with a negative index metamaterial. *Nano Lett.* **9,** 3565–3569 (2009).
24. Atkinson, R. *et al.* Anisotropic optical properties of arrays of gold nanorods embedded in alumina. *Phys. Rev. B* **73,** 235402 (2006).
25. Dickson, W. *et al.* Dielectric-loaded plasmonic nano-antenna arrays: a metamaterial with tuneable optical properties. *Phys. Rev. B* **76,** 115411 (2007).
26. Evans, P. R. *et al.* Plasmonic core/shell nanorod arrays: sub-atto-liter controlled geometry and tunable optical properties. *J. Phys. Chem. C* **111,** 12522–12527 (2007).
27. Wurtz, G. A. *et al.* Guided plasmonic modes in nanorod assemblies: strong electromagnetic coupling regime. *Opt. Express* **16,** 7460–7470 (2008).
28. Evans, P. *et al.* Growth and properties of gold and nickel nanorods in thin film alumina. *Nanotechnology* **17,** 5746–5753 (2006).
29. Bigot, J.-Y., Halte, V., Merle, J.-C. & Daunois, A. Electron dynamics in metallic nanoparticles. *Chem. Phys.* **251,** 181–203 (2000).
30. Rosei, R. & Lynch, D. W. Thermomodulation spectra of Al, Au, and Cu. *Phys. Rev. B* **5,** 3883–3894 (1972).
31. Sönnichsen, C., Franzl, T., Wilk, T., von Plessen, G. & Feldmann, J. Drastic reduction of plasmon damping in gold nanorods. *Phys. Rev. Lett.* **88,** 077402 (2002).
32. Maier, S. A. *et al.* Plasmonics—a route to nanoscale optical devices. *Adv. Mater.* **13,** 1501–1506 (2001).


## Acknowledgements

The work of G.A.W., R.P., W.H. and A.V.Z. was supported by the Engineering and Physical Sciences Research Council (EPSRC) (UK). G.P.W. and D.J.G. were supported through the Center for Nanoscale Materials by the US Department of Energy, Office of Science, Office of Basic Energy Sciences (contract no. DE-AC02-06CH11357). The work of V.A.P. was supported by the National Science Foundation (ECCS-0724763) and the Office of Naval Research (N00014-07-1-0457).

## Author contributions

G.A.W. and A.V.Z. conceived and designed the experiments. G.A.W., G.P.W. and D.J.G. performed the experiments. R.P. and W.H. fabricated samples. G.A.W. G.P.W., V.A.P. and A.V.Z. analysed the data and co-wrote the paper. All authors discussed the results and commented on the manuscript.

## Additional information

The authors declare no competing financial interests. Supplementary information accompanies this paper at www.nature.com/naturenanotechnology. Reprints and permission information is available online at http://npg.nature.com/reprintsandpermissions/. Correspondence and requests for materials should be addressed to A.V.Z.